Biogeosciences Discuss., 9, 13351–13396, 2012
www.biogeosciences-discuss.net/9/13351/2012/
doi:10.5194/bgd-9-13351-2012

Biogeosciences Discussions

Isoprene emissions from a tundra ecosystem

M. J. Potosnak[1], B. M. Baker[2], L. LeStourgeon[1], S. M. Disher[2], K. L. Griffin[3], and M. S. Bret-Harte[4]

[1]Department of Environmental Science and Studies, DePaul University, Chicago, Illinois, USA
[2]Department of Chemistry, California State University-Sacramento, Sacramento, California, USA
[3]Lamont-Doherty Earth Observatory of Columbia University, Palisades, New York, USA
[4]Institute of Arctic Biology, University of Alaska-Fairbanks, Fairbanks, Alaska, USA

Received: 7 September 2012 – Accepted: 10 September 2012 – Published: 1 October 2012

Correspondence to: M. J. Potosnak (mpotosna@depaul.edu)

Published by Copernicus Publications on behalf of the European Geosciences Union.

Abstract

Whole-system fluxes of isoprene from a moist acidic tundra ecosystem and leaf-level emission rates of isoprene from a common species (*Salix pulchra*) in that same ecosystem were measured during three separate field campaigns. The field campaigns were conducted during the summers of 2005, 2010 and 2011 and took place at the Toolik Field Station (68.6° N, 149.6° W) on the north slope of the Brooks Range in Alaska, USA. The maximum rate of whole-system isoprene flux measured was over 1.2 mg C m^{-2} h^{-1} with an air temperature of 22 °C and a PAR level over 1500 µmol m^{-2} s^{-1}. Leaf-level isoprene emission rates for *S. pulchra* averaged 12.4 nmol m^{-2} s^{-1} (27.4 µg C gdw^{-1} h^{-1}) extrapolated to standard conditions (PAR = 1000 µmol m^{-2} s^{-1} and leaf temperature = 30 °C). Leaf-level isoprene emission rates were well characterized by the Guenther algorithm for temperature, but less so for light. Chamber measurements from a nearby moist acidic tundra ecosystem with less *S. pulchra* emitted significant amounts of isoprene, but at lower rates (0.45 mg C m^{-2} h^{-1}). Comparison of our results to predictions from a global model found broad agreement, but a detailed analysis revealed some significant discrepancies. An atmospheric chemistry box model predicts that the observed isoprene emissions have a significant impact on Arctic atmospheric chemistry, including the hydroxyl radical (OH). Our results support the prediction that isoprene emissions from Arctic ecosystems will increase with global climate change.

1 Introduction

Emission of biogenic volatile organic compounds (BVOCs) from plants strongly couples terrestrial ecosystem processes and atmospheric chemistry cycles, and the cross-disciplinary nature of this subject brings together the fields of ecophysiology, plant physiology, ecology, micrometeorology, and atmospheric chemistry. While the functions of some BVOCs are now well understood – ranging from protection against herbivory

BGD
9, 13351–13396, 2012

(monoterpenes; Trapp and Croteau, 2001) to by-products of plant growth (methanol; Fall, 2003) – the function of another important BVOC, isoprene, is still debated (Sharkey and Singsaas, 1995; Rosenstiel et al., 2004; Loreto et al., 2001). This study focuses on isoprene (C_5H_8), which accounts for 500 to 750 Tg of carbon emitted globally (Guenther et al., 2006). Once BVOCs enter the atmosphere, they have profound effects on regional air quality (Chameides et al., 1988), the global oxidizing capacity of the atmosphere (Crutzen and Zimmermann, 1991), and secondary organic aerosol production (Andreae and Crutzen, 1997). BVOC emissions are also sensitive to climate change (Lathiere et al., 2010; Penuelas and Staudt, 2010). Examples of factors affected by climate change which impact ecosystem isoprene production are species composition (Sharkey and Yeh, 2001), temperature (Monson and Fall, 1989; Sharkey et al., 1999), nitrogen availability (Harley et al., 1994), and canopy architecture (Harley et al., 1996; Baldocchi et al., 1999).

Most field studies of isoprene emissions have focused on temperate ecosystems (e.g. Goldstein et al., 1995; Pressley et al., 2005; McKinney et al., 2011) due to accessibility and tropical ecosystems (e.g. Geron et al., 2002; Rinne et al., 2002; Langford et al., 2010) because warm temperatures, high biomass densities, and long growing seasons drive globally significant fluxes. Other studies have stretched from savannahs (e.g. Guenther et al., 1996; Otter et al., 2003) to boreal forests (e.g. Rinne et al., 2000; Spirig et al., 2004). However, Arctic (latitude above 66.6° N) tundra ecosystems have been neglected, with only 4 studies coming from the same field station near Abisko, Sweden (Ekberg et al., 2009; Faubert et al., 2010; Rinnan et al., 2011; Tiiva et al., 2008) and another study in northern Finland (Tiiva et al., 2007).

The Arctic is an important region to observe ecosystem responses to global climate change. Observations and model predictions both indicate that high-latitude ecosystems are particularly sensitive to global climate change for two reasons. First, the climate of the Arctic is disproportionately affected by global climate change. For example, CO_2 concentration measurements have revealed increases in growing-season length (Myneni et al., 1997), and temperature records (including paleoclimate proxies)

BGD
9, 13351–13396, 2012

have revealed a strong warming trend at high latitudes (Overpeck et al., 1997; Serreze et al., 2000). Precipitation amounts also have increased during the last 50 years (Rawlins et al., 2010). Unique aspects of the Arctic climate system also contribute to increased sensitivity to climate change. The recent precipitous decline in sea-ice extent (Kwok et al., 2009) also highlights the sensitivity of the Arctic region to global change. Changes in surface temperature, ice sheets, glaciers, snow cover, permafrost, and sea ice are detectable through satellite observations (Comiso and Parkinson, 2004). Additionally, many climate models predict a decrease in thermohaline circulation, which impacts the heat budget of vast regions of the Arctic (Clark et al., 2002). Finally, Arctic warming trends drastically change the state of an ecosystem by eroding the permafrost layer and increasing active layer depth (Chen et al., 2003; Frauenfeld et al., 2004).

The second reason driving the sensitivity of the region to global climate change is that Arctic ecosystems are highly adapted to extreme environmental conditions and small environmental changes may have large consequences. For example, if a perturbation in Arctic climate causes an increase in deciduous shrubs, the "snow fence" effect will cause greater snow depths leading to warmer soil temperatures, increased mineralization rates, and more nutrient availability – which favours further shrub growth (Sturm et al., 2001). This positive feedback loop demonstrates the inherent instability of the tundra ecosystem in regard to climate change.

1.1 Previous research on Arctic air-surface exchanges

Previous field studies have explored aspects of the impact of surface exchanges with the terrestrial biosphere on atmospheric chemistry in high-latitude regions, but there has been little focus on summer-time BVOC chemistry. The Arctic Boundary Layer Expedition (ABLE-3A) focused on investigating exchange processes of NO_y, CO, and methane on the ground in the Yukon-Kuskokwim Delta region. These ground-based experiments were complemented by airborne measurements of a variety of important reactive trace gases (Harriss et al., 1992b). While detailed knowledge of methane sources and sinks (Bartlett et al., 1992) as well as NO_x (Bakwin et al., 1992) and O_3

BGD
9, 13351–13396, 2012

deposition fluxes (Jacob et al., 1992) were obtained during ABLE-3A, BVOC exchange measurements were not quantified. Non-methane hydrocarbon measurements on the NASA Electra research aircraft, however, indicated the abundance of important biogenic reactive trace gases in the Arctic (isoprene, Blake et al., 1992).

In contrast to the terrestrial biosphere, many studies have focused on the impact of ice and snow surfaces on Arctic atmospheric chemistry. These studies were motivated by the observation that these air-surface exchanges had important implications for cycles of atmospheric chemistry in the Arctic. One emphasis has been springtime O_3 depletion events (Barrie et al., 1988), which are observed throughout the Arctic at coastal stations (Helmig et al., 2007). Arctic O_3 depletion is thought to be linked to emissions of halogens from sea ice (Helmig et al., 2007). In addition, a significant amount of data has been collected above the snowpack and firn ice with important implications for Arctic photochemistry. These investigations were prompted by the finding from the Polar Sunrise Experiment (PSE98) that formaldehyde was emitted from the snowpack at Alert after polar sunrise (Sumner and Shepson, 1999; Sumner et al., 2002). The impact of air-ice exchanges on Arctic atmospheric chemistry demonstrates the sensitivity of the system to relatively small exchanges of reactive species.

1.2 Previous research on global change factors and deciduous shrub species

The Toolik Field Station (TFS) has been the setting for a wide variety of ecological experiments focused on global change factors in the Arctic. Most of the global change factor experiments conducted at TFS fall into three categories: fertilization, warming, and shading (including interactions among these factors). Shaver et al. (2001) found that *Betula nana*, a deciduous species (dwarf birch), dominated the upper canopy when nutrients were added to a moist acidic tundra ecosystem. The fertilization effect can become self-sustaining since leaf litter from *B. nana* is more readily decomposable (van Wijk et al., 2004). In comparison, for sites where deciduous species had a relatively low starting percentage of cover (i.e. moist non-acidic tundra), deciduous shrub cover did not increase with either fertilization or warming (Gough and Hobbie, 2003). Warming

BGD
9, 13351–13396, 2012

experiments showed species responses that favoured deciduous plants (Hobbie and Chapin, 1998) in moist acidic tussock tundra, while shading experiments led to decreased shrub growth (Chapin et al., 1995). Another snow-depth study found that either increased soil temperatures (due to direct warming) or drifting snow lead to increases in growing season length and greater biomass (Walker et al., 1999) for both moist and dry ecosystem types. This predicted increase in the dominance of shrubs has been seen in aerial photographs (Tape et al., 2006), detected in the Russian Arctic using tree-ring growth (Forbes et al., 2010) and is the current focus of remote sensing studies (e.g. Boelman et al., 2011). Increases in deciduous shrubs could lead to increases in ecosystem BVOC emissions, since shrubs have higher emission capacities than grasses and sedges (Guenther et al., 2006).

1.3 Current study

The current study investigates two hypotheses. *The first is that isoprene emissions from tundra ecosystems have a significant impact on Arctic atmospheric chemistry.* As outlined above, previous Arctic atmospheric chemistry studies show the system is sensitive to air-surface interactions over snow and seawater. Our studies use leaf-level and whole-system measurements of isoprene emission from a moist acidic tundra ecosystem to estimate ecosystem emission factors. First, we compare these measured factors to a global isoprene model. Next, these factors are then used to drive an atmospheric chemistry model to determine their impact on Arctic photochemistry. *Our second hypothesis is that global change factors will lead to increased future isoprene emissions.* If isoprene emissions from deciduous shrubs play a key role in the current system, this influence is predicted to grow with the increasing dominance of tundra shrubs which could result from warming Arctic temperatures. We test this hypothesis by performing leaf-level isoprene emission rate measurements at an existing experiment that manipulates nutrients and ecosystem temperature. To support the exploration our hypotheses outlined above, we also have the goal of testing the applicability for Arctic tundra

BGD
9, 13351–13396, 2012

species and ecosystems of leaf-level and whole-system models of isoprene emission that were primarily developed based on observations from mid-latitude species.

2 Methods

2.1 Overview of field campaigns

All research was performed near the Toolik Field Station (68° 38′ N, 149° 38′ W) on the north slope of the Brooks Range in Alaska (Fig. 1) in moist acidic tundra ecosystems. Data were collected during 3 field campaigns that occurred near the peak of the growing season in late June and early July for the years 2005, 2010 and 2011. The eddy covariance technique was used during 2005 and 2010 (denoted as EC05 and EC10) to measure isoprene fluxes at an existing station that measures carbon dioxide (CO_2) flux. This station is located in the Imnavait Creek experimental watershed, which is 12 km east of the main field station (labelled EC in Fig. 1), and is at an elevation of 930 m. The existing eddy flux system is part of the Arctic Observatory Network (http://aon.iab.uaf.edu, Euskirchen et al., 2012). Whole-system measurements of isoprene fluxes were also obtained with static and dynamic chamber systems during 2011 (CH11) at a location approximately 500 m north of the main field station (labelled CH in Fig. 1). The leaf-level data were also collected during the 2011 field campaign from and near an existing global change manipulation experiment (labelled LL in Fig. 1).

2.2 Leaf-level measurements

Leaf-level measurements were performed with a LI-6400 leaf-gas exchange system (LI-COR Biosciences, Lincoln, Nebraska, USA) with a self-contained LED light source and typical gas-exchange parameters were measured (e.g. photosynthesis, transpiration, conductance and intercellular CO_2 concentration). The system has the ability to control leaf temperature, incident light and CO_2 concentration of the incoming air stream. There is some ability to control water vapour via a desiccant scrub (Drierite,

BGD
9, 13351–13396, 2012

W.A. Hammond Drierite, Xenia, Ohio, USA) or by adding < 10 ml of water to the CO_2 scrub (soda lime). Incoming air first was drawn though an external filter to remove hydrocarbons and ozone (Refillable Hydrocarbon Trap, Restek, Bellefonte, PA). If CO_2 was being controlled, the built-in CO_2 scrubber removed all incoming CO_2 and the LI-6400 mixer set the concentration using disposable CO_2 cartridges (LI-COR).

Isoprene emission rates were determined by measuring the isoprene concentration of air exiting the LI-6400. Two methods were employed to measure the isoprene concentration, and both were based on solid absorbents and analysis by gas chromatograph with a flame ionization detector (GC-FID). In the first method, solid absorbent cartridges were filled in the field and then analysed in the laboratory. For the second method, the exhaust stream was coupled to an automated GC-FID with a fixed solid absorbent trap.

For measuring isoprene from the chamber systems and the LI-6400, isoprene samples were collected on solid absorbent cartridges (6.4 mm (1/4 in) O.D. stainless-steel tubes filled with Tenax TA, Carbotrap and Carboseive) and analysed on a GC-FID (SRI Instruments, Torrance, California, USA). A battery powered pump (SKC, Eighty Four, Pennsylvania, USA) was used to draw a known amount of air through the solid absorbent cartridges. The GC-FID has a custom-designed preconcentration system using a solid absorbent bed (Tenax TA and Carbotrap). The system was calibrated by running cartridges filled with a known standard that were brought to the Toolik Field Station. Isoprene identification was confirmed by sending a subset of duplicate sample cartridges to the laboratory for GC-MS (gas chromatograph-mass spectrometer) analysis (HP5890/5971, Hewlett-Packard, Palo Alto, California, USA). For transport of the prefilled standard cartridges to Toolik and the return of the cartridges for GC-MS analysis, the cartridges were kept refrigerated (typically 4 °C) for a majority of the time.

The second method of determining the isoprene concentration of air exiting the LI-6400 system was an online GC-FID. The GC system is more fully described in Papiez et al. (2009). Briefly, isoprene was concentrated on a fixed Tenax-TA (60/80 mesh) trap made from 3.2 mm (1/8 in) O.D., 2.16 mm (0.085 in) I.D. fused-silica-lined stainless

BGD
9, 13351–13396, 2012

steel tubing. After an automated valve was switched, the trap was heated to 200 °C and the sample injected into the column (0.53 mm I.D. by 30 m, 3.0 µm film MXT-624 capillary column, Restek). The oven temperature program was 2 min at 50 °C followed by a 15 °C min^{-1} ramp to 200 °C. The gas chromatograph was similar to the one employed for cartridge-based measurements (model 8610C, SRI). Calibration was performed by a cross comparison to the other GC-FID system. The calibration was checked with a gas-phase standard containing isoprene from Scott-Marrin, Inc. (Riverside, California, USA) upon return to Chicago. This on-line system had the advantage of performing a series of automated measurements when coupled to the LI-6400. For the campaigns in years 2005 and 2011, the GC-FID was transported to the Imnavait Creek flux tower and powered by the gasoline generator. In these cases, measurements were made on intact leaves. In 2011, measurements were also made on excised leaves in the laboratory. Investigators have done photosynthetic and respiratory experiments on excised leaves of *S. pulchra* from this tundra ecosystem, and comparisons have shown no effect of excision at times up to 2 h (data not shown). In addition, a comparison of excised leaves and intact leaves conducted at Imnavait Creek showed no significant difference in emission rates (data not shown).

Temperature and light curves were obtained by using an autoprogram with a 20-min time step. For temperature curves, leaf temperature was first set to 30 °C, and then stepped from 20 to 32.5 in 2.5 °C increments. For light curves, PAR (photosynthetically active radiation) was initially set to 1000 µmol m^{-2} s^{-1}, and then stepped through 100, 200, 400, 800, 1000 and 1600 µmol m^{-2} s^{-1}. For the temperature curves, light was kept constant at 1000 µmol m^{-2} s^{-1} and for the light curves, leaf temperature was kept at 25 °C. For all measurements, flow rate was constant at 250 µmol s^{-1} and incoming CO_2 was controlled at 400 ppmv. When ambient humidity was low, drops (< 10 ml) of distilled water were added to the CO_2 scrub to minimize the leaf vapour pressure deficit.

The measured responses were compared to predictions based on the algorithms proposed by Guenther et al. (1993), commonly known as the Guenther algorithms.

BGD
9, 13351–13396, 2012

Leaf-level emissions are predicted by

$$\text{Emission}_{\text{leaf}} = \text{EF}_{\text{leaf}} \times C_{\text{L}} \times C_{\text{T}} \quad (1)$$

were EF_{leaf} is the basal emission rate at 30 °C leaf temperature and 1000 µmol m^{-2} s^{-1} PAR. The two factors are

$$C_{\text{L}} = \frac{\alpha C_{\text{L1}} L}{\sqrt{1 + \alpha^2 L^2}} \quad (2)$$

where $\alpha = 0.0027$, $C_{\text{L1}} = 1.066$, and L is the PAR level, and

$$C_{\text{T}} = \frac{\exp \frac{C_{\text{T1}}(T - T_{\text{S}})}{RT_{\text{S}}T}}{1 + \exp \frac{C_{\text{T2}}(T - T_{\text{M}})}{RT_{\text{S}}T}} \quad (3)$$

where $R = 8.314\,\text{J K}^{-1}\,\text{mol}^{-1}$, $C_{\text{T1}} = 95\,000\,\text{J mol}^{-1}$, $C_{\text{T2}} = 230\,000\,\text{J mol}^{-1}$, $T_{\text{S}} = 303\,\text{K}$, $T_{\text{M}} = 314\,\text{K}$, and T is the leaf temperature in K.

For light curves, the measured emissions in each curve were normalized by the measurement taken at PAR = 1000 µmol m^{-2} s^{-1}. For temperature curves, the instrument was not always able to obtain the leaf temperature set point, so measurements were normalized by calculating the slope of a linear fit of measured emissions versus calculated C_{T} values. The slope was then used to normalize the measurements.

A simplified linear relationship between light and emissions was also explored

$$C_{\text{LLinear}} = \frac{L}{L_{\text{S}}} \quad (4)$$

where $L_{\text{S}} = 1000\,\mu\text{mol m}^{-2}\,\text{s}^{-1}$.

BGD
9, 13351–13396, 2012

2.3 Global change experiment

We performed leaf-level isoprene emission rate measurements on *S. pulchra* plants from an existing global change manipulation experiment (for full details, see Chapin et al., 1995; Bret-Harte et al., 2001; Shaver et al., 2001). The following treatments were applied in addition to the control (C): nitrogen (N), phosphorus (P), combined nitrogen and phosphorus (NP), and a greenhouse (GH) treatment which elevated ecosystem temperature. Each treatment was applied to a 5 by 20 m plot and replicated in 4 blocks. The fertilization plots (N, P, NP) received the respective treatments of fertilizer after snowmelt each June. The greenhouses were simple wooden "A" frames, approximately 2 by 4 m and are covered annually with 0.15 mm transparent plastic sheeting in late May and uncovered at the end of August (Bret-Harte et al., 2001). PAR was reduced in the greenhouse due to the plastic sheeting by about 20 % of the ambient light PAR values (data not shown). Air temperature and relative humidity were also measured during the growing season with sensors read every minute and averaged every hour. During the summer months, the daytime air temperature within the greenhouses typically ranged 5–10 °C warmer than the ambient air temperatures. The data were analysed using Tukey's Honest Significant Difference (HSD) test.

2.4 Eddy covariance measurements

For EC05 and EC10, we used the eddy covariance (EC) technique to measure canopy-level fluxes. The eddy covariance technique requires that the landscape is homogeneous (Baldocchi, 2003), and the long-term record of CO_2 fluxes, including turbulence data, is useful for testing this assumption. CO_2 fluxes obtained at this site were well described by an ecosystem model using an ensemble Kalman filter (Rastetter et al., 2010). Ecosystem fluxes were calculated with standard micrometeorological procedures closely related to basic protocols used for analysing eddy covariance data developed by the flux community for the EUROFLUX (now known as CARBOEUROPE) (Aubinet et al., 2000) and AmeriFlux networks (Baldocchi et al., 2001). Wind and

BGD
9, 13351–13396, 2012

isoprene concentration measurements were recorded at a rate fast enough (10 and 1 Hz, respectively) to capture all changes in air motion which significantly contribute to the flux. Isoprene fluxes were determined directly by using a Fast Isoprene System (FIS) analyser (Guenther and Hills, 1998) from Hills Scientific (Boulder, Colorado, USA). This instrument uses a chemiluminescence technique to measure isoprene by counting photons from the reaction of O_3 (generated by the system) and isoprene. Isoprene flux measurements were conducted at the existing CO_2/H_2O eddy covariance tower. The AON project provided all ancillary measurements (e.g. radiation, air temperature) necessary for interpreting our isoprene flux measurements.

A description of the eddy covariance equipment and data analysis procedures for the CO_2 and H_2O fluxes is given in Rastetter et al. (2010) and is briefly summarized here. Eddy covariance data were collected with an open-path CO_2/H_2O gas analyser (LI-7500, LI-COR) and sonic anemometer (CSAT3, Campbell Scientific, Logan, Utah, USA) located approximately 2 m above the land surface. The vertical wind was rotated using the 2-D method of Wilczak et al. (2001) and the derived rotation angles closely matched the slope (cf. Turnipseed et al., 2003, Fig. 7). After computing the covariance between the rotated wind and the CO_2 concentrations, the CO_2 fluxes were corrected using the sensible and latent heat fluxes (Webb et al., 1980). Isoprene fluxes were calculated in a similar manner with two exceptions. First, the FIS instrumental noise restricted the collection frequency to 1 Hz, so the wind measurements were averaged to that frequency. Second, because of relatively low isoprene concentrations, the corrections of Webb et al. (1980) are small and were neglected.

Although the existing flux tower was powered by solar panels and a wind turbine, because of power requirements the FIS was run using a portable gasoline generator (2 kVA). For EC05, the generator was located approximately 100 m from the tower, in the prevailing down-wind direction. For EC10, the generator was located approximately 300 m down slope (towards the west).

BGD
9, 13351–13396, 2012

2.5 Whole-system emission models

Whole-system isoprene emissions were modelled with two methods. First, for the chamber measurements and for the eddy covariance data, a big-leaf model analogous to Eq. (1) was used

$$\text{Emission}_{\text{canopy}} = \text{EF}_{\text{canopy}} \times C_{\text{L}} \times C_{\text{T}} \quad (5)$$

The only change compared to Eq. (1) is that air temperature was used in place of leaf temperature. Also, we explored using $C_{\text{L Linear}}$ in place of C_{L} for the whole-system data.

Equation (5) was used to infer the canopy emission factor from the whole-system measurements. Equation (5) was rearranged to solve for $\text{EF}_{\text{canopy}}$ based on the measured values of $\text{Emission}_{\text{canopy}}$ and values of C_{L} and C_{T} based on ambient light and temperature for each 30-min flux period. The approach uses several assumptions to allow the use of these leaf-level equations. First, air temperature is used in place of the leaf temperature. Second, the canopy is treated as a single flat leaf with a leaf area index (LAI) equal to 1. By plotting observed emissions against the combined temperature and light scaling factors, the canopy emission factor is derived from the slope of the best fit line with a zero intercept. We also employed the MEGAN framework (Model of Emissions of Gases and Aerosols from Nature) described in Guenther et al. (2006). The model employs a radiative transfer scheme to predict incident light for both sun and shade leaves with a 5-layer canopy. In addition, the model calculates leaf temperature accounting for air temperature, vapour pressure deficit and wind speed. The model uses the following meteorological variables from the existing eddy flux system: solar radiation, air temperature, absolute humidity and wind speed. The only other parameters necessary for MEGAN are LAI, which was set to 0.66 following Williams et al. (2006), latitude (68.5° N) and canopy type (grass). The MEGAN approach is similar to Eq. (5)

$$\text{Emission}_{\text{canopy}} = [\varepsilon][\gamma] \quad (6)$$

BGD
9, 13351–13396, 2012

where ε is a canopy emission factor analogous to EF_{canopy} in Eq. (5) and γ depends on the meteorological variables.

We used a transect method to estimate the ecosystem LAI for *S. pulchra* surrounding the tower, the focus of our leaf-level measurements. Starting 10 m from the base of the tower, we used existing transects that followed the 4 cardinal directions. Each transect ranged from 10 to 45 m and each point in the transect was spaced at 5 m. For each point in the transect, we counted the number of branches of *S. pulchra* within a 30 cm radius. A random sub-sample of branches was collected and leaf area per branch was determined with a flatbed scanner. The average leaf area per branch was then used to scale up the number of branches at each transect location, which was then averaged to estimate an ecosystem-level LAI for *S. pulchra*.

2.6 Chamber measurements

For CH11, two chamber systems were used to measure isoprene fluxes: a larger static chamber and a smaller dynamic chamber. The static measurements were made with a rigid plastic chamber that fitted to pre-existing plastic square bases inserted into the soil. The chamber was approximately 35 cm in height (including the base) and 1.2 m on each side, enclosing a ground-surface area of 1.46 m^2. The bases were installed for a project measuring whole-system CO_2 isotopes (Greg Starr, 2012, personal communication). A static chamber technique was employed with 4 box fans in the chamber to promote mixing. A series of 3–4 cartridge samples were collected over 15 to 20 min to calculate the change in isoprene concentration with time. Static chambers have the disadvantage of perturbing environmental conditions, and in particular lead to increasing air and leaf temperatures (Ortega and Helmig, 2008). To compensate for this, air temperature was continuously monitored with a thermocouple inside the chamber and light with a PAR sensor (model MQ, Apogee Instruments, Logan, Utah, USA). Also, immediately after removing the chamber, leaf/ground temperatures were measured with an infrared thermometer inside and outside the chamber base to assess the impact of heating.

BGD
9, 13351–13396, 2012

In addition, leak rates were significant, since isoprene concentrations inside the chamber were much higher than outside concentrations (typically by a factor of 100). High chamber concentrations can lead to an underestimate of flux rates with the static enclosure technique (Nay et al., 1994). We used a simple model to predict the ecosystem exchange factor (EF_{canopy}) using Eq. (5) and a leak rate. The leak rate was estimated to be 7 % min^{-1} based on measuring the decay rate of isoprene when the chamber was covered with a tarp. The model predicted isoprene concentrations with a one-minute time step by using Eq. (5) to estimate emissions and then accounting for the loss of isoprene due to the leak rate. The basal emission rate was determined iteratively by minimizing the residual sum of squares calculated from the measured isoprene concentrations.

Dynamic chamber measurements were also employed with smaller chambers. Again, these chambers had pre-existing bases. The smaller chambers were circular, with a diameter of 19.2 cm and an enclosed surface area of 290 cm^2. The flow rate through the chamber was 0.9 l min^{-1}. Fluxes were calculated by measuring the isoprene concentration of air exiting the chamber and subtracting the concentration of isoprene measured in ambient air entering the chamber. Temperature and light were measured with the same equipment described for the static chambers.

2.7 Atmospheric chemistry model

The impact of isoprene emissions on Arctic atmospheric chemistry was investigated with the RACM2 model (Regional Atmospheric Chemistry Mechanism, version 2, Stockwell and Goliff, 2004; Papiez et al., 2009). By running RACM with and without isoprene emissions and observing how the predicted concentrations of reactive species varied with time, we could assess how isoprene emissions influence atmospheric chemistry. This model includes a comprehensive isoprene oxidation scheme and lumps chemical species together for computational efficiency. The RACM2 mechanism was used in a box model mode, assuming a fixed convective boundary layer

BGD
9, 13351–13396, 2012

(CBL) height of 1000 m. The model has zero spatial dimensions, so the CBL height is only used for the dilution of the isoprene emission source. Measurements at a similar latitude found a CBL height of 750 m (Liberto et al., 2012), and using 1000 m provides a lower-bound estimate on the impact of isoprene on chemical processes. The model output step was 30 min and ran from 07:00 to 01:00 the following day, local Alaska Daylight Time. Photolysis rates used for driving the model chemistry were generated using the appropriate time, date and latitude with the assumption of clear-sky conditions. Isoprene was added for each 30 min time step using emissions observed during day 180 of EC05. The model was also run with these emissions set to zero to analyse the impact of emissions on chemical processes. The initial concentrations of reactive gases were selected based on observations obtained during the ABLE 3A study (Table 1), primarily near Barrow, Alaska.

3 Results and discussion

3.1 Leaf-level emission rates

3.1.1 Temperature and light response

Leaf-level rates of isoprene emission were explored as a function of leaf temperature and light (Fig. 2). We used Eq. (1) to compare our measurements to predictions from the well-tested algorithms of Guenther et al. (1993). No adjustments were made to the coefficients of the published algorithm. The fit to temperature is good, with the algorithm explaining 96 % of the observed variation (Fig. 2, left panel). The fit for light was less satisfactory and only 58 % of the variation was explained. The response to light is more linear than predicted by the algorithm, which also has been observed in tropical ecosystems (Keller and Lerdau, 1999). A simple linear relationship using a zero intercept constrained to a factor of 1 at a PAR = 1000 $\mu mol\,m^{-2}\,s^{-1}$ (Eq. 4) explains 64 % of the variance, a slight improvement.

BGD
9, 13351–13396, 2012

Our next goal was to determine the average basal emission rate (EF_{leaf} in Eq. 1) for *S. pulchra*. We measured 21 independent leaves from a location approximately 500 m southwest of the field station. These leaves were located in the control plots of an experiment to measure the impact of nutrient addition and warming on the tundra ecosystem (Chapin et al., 1995). The average emission rate from these measurements at a leaf temperature of 25 °C and 1000 µmol m^{-2} s^{-1} PAR was 6.85 (SD = 5.87) nmol m^{-2} s^{-1}. Using measured dry leaf mass to express this on a gram dry weight (gdw) basis, the average rate is 15.1 µg C gdw^{-1} h^{-1}. Since the Guenther algorithm for temperature worked well with our dataset, we can use Eq. (3) to estimate the rate at 30 °C to be 27.4 µg C gdw^{-1} h^{-1} to compare our results to measurements from temperate ecosystem plants. Our measured rate is very close to the average (27.2 µg C gdw^{-1} h^{-1}) which has been previously reported in the BVOC emission inventory for all *Salix* species (Wiedinmyer, 2004). Overall, the leaf-level isoprene emissions from *S. pulchra* located in the moist acidic tundra ecosystem were consistent with previous results from mid-latitude ecosystems, except that the response to light was more linear than predicted.

3.1.2 Global change factor experiment

There were no significant differences observed in leaf-level isoprene emission rates from *S. pulchra* for any of the nutrient addition experiments versus the control: $p = 0.98$ for N, $p = 0.98$ for P and $p = 0.99$ for NP. This was contrary to our expectation, since in particular nitrogen fertilization has been shown to increase isoprene emission rates for temperate species (Harley et al., 1994). Our results are consistent with a recent report that also found no impact of fertilization on isoprene emissions from a similar *Salix* species (*S. phylicifolia*) treated to a similar fertilization experiment in Abisko, Sweden (Rinnan et al., 2011). On the other hand, the greenhouse warming experiment lead to an over 3-fold increase in isoprene emission rates: from 4.49 to 13.92 nmol m^{-2} s^{-1}, $p = 0.0000035$. This result is consistent with many previous studies on the impact of growth temperature on the isoprene emission capacity of plants (for an early reference,

BGD
9, 13351–13396, 2012

see Monson and Fall, 1989). Unlike the fertilization component, our results differ from the similar experiment performed in Sweden (Rinnan et al., 2011). Rinnan et al. observed no significant difference for the warming treatment on *S. phylicifolia*. Three observations may explain this discrepancy. (1) In the Sweden experiment, by chance weather changes caused the temperatures in the warmed plot to be the same as the control plot at the time of measurement. Although our protocol of using detached leaves makes the instantaneous temperature the same (25 °C), short-term effects (5 to 10 days) could be influencing the basal emission rate (Petron et al., 2001) in our results. (2) The amount of warming in the two experiments differed. In our experiment, air temperatures were elevated in the range of 5 to 10 °C, while in the Sweden experiment the average was 4 °C (see Sect. 2.1 in Rinnan et al., 2011). (3) The statistical power in the Sweden experiment is relatively low ($n = 3$), and true differences in the mean may have been masked by high variability (see Table 2 in Rinnan et al., 2011).

3.2 Whole-ecosystem emissions

3.2.1 Eddy covariance measurements

We measured whole-system isoprene fluxes at the Imnavait Creek field site during the summer of 2005 (EC05) and we observed fluxes exceeding 1.2 mg C m^{-2} h^{-1} on day 180 (29 June) (Fig. 3). To put this in perspective, a northern hardwood forest in Michigan had average midday fluxes of 3 mg C m^{-2} h^{-1} over the entire growing season (Pressley et al., 2005), and several short datasets of emissions from tropical ecosystems give estimates of approximately 2.5 mg C m^{-2} h^{-1} (Rinne et al., 2002; Karl et al., 2004). This tundra ecosystem has a much lower LAI than both the mid-latitude and tropical forested ecosystems. In addition, the average daily temperatures during the growing season are also much lower for tundra ecosystems. Lower LAI and lower average temperature are factors that decrease whole-system isoprene emissions (Guenther et al., 2006).

BGD
9, 13351–13396, 2012

The record from EC05 is relatively short since this was an exploratory experiment and logistics constrained the amount of data collected. In addition, after day 180 the weather turned much cooler: air temperature did not exceed 10 °C for the following week. This cool weather prevented further meaningful flux measurements. As seen on day 182, these low temperatures completely suppress isoprene emissions, even though light levels exceeded 1500 $\mu mol\, m^{-2}\, s^{-1}$. This result is expected, since Eq. (2) decreases by a factor of 4 when the temperature decreases from 20 to 10 °C. Given the short span of our experiment, we did capture one of the warmest days of the growing season. Only for two consecutive days in August did air temperature exceed the level reached on day 180.

For EC10, one day (190) had temperatures that exceeded 20 °C and were similar to day 180 in EC05 (Fig. 4). In this case, isoprene emission fluxes reached over 0.8 $mg\, C\, m^{-2}\, h^{-1}$. Because of the short nature of both datasets, we cannot determine if this difference represents experimental error or a true difference in the underlying capacity of the ecosystem to emit isoprene. From the experimental error perspective, estimation of sensible and latent heat fluxes by the eddy covariance can be off by 20 % (Goulden et al., 1996). This should be considered a lower bound for the error in our isoprene fluxes, and could potentially explain half of the observed difference between EC05 and EC10.

But given the uncertainty in our measurements due to their limited length, the change in observed emission rates at similar conditions for light and temperature could be due to preceding air temperatures. The capacity to emit isoprene (EF_{leaf} in Eq. 1) varies with the previous temperature experienced by leaves. For oaks, Petron et al. (2001) observed that isoprene emission at a leaf temperature of 30 °C doubled when the growth temperature increased from 25 to 30 °C. In EC05, the maximum temperature increased linearly from 13 to 20 °C in the 5 days preceding day 180. In EC10, although the air temperature reached almost 20 °C on the day previous to 190, the temperature had not exceeded 10 °C in the 3 days previous to that (days 186–188, Fig. 4).

BGD
9, 13351–13396, 2012

MEGAN uses two time periods to model the impact of previous temperature: 1 day and 10 days. Using these metrics, EC05 and EC10 are similar. For the previous 1 day, the average temperature was 16.8 °C in 2005 and 19.0 °C in 2010, while for the previous 10 days, the averages were 10.5 °C (2005) and 10.4 °C (2010). The algorithm in MEGAN would predict a 12 % higher emission capacity in 2010 compared to 2005 because of the 2.2 °C increase in averaged air temperature over the preceding 1 day, while the small 0.1 °C change over the preceding 10 days results in a change of less than 1 %. The predicted 12 % increase is opposite of the observed decrease in emissions from 2005 to 2010 under similar temperature and light conditions. But as mentioned above, the air temperatures in 2010 were much cooler 2 days before the warm day. Using 5 days as the averaging period, in 2005 the average temperature was 14.9 °C while it was 9.7 °C in 2010. Again, no conclusions can be drawn from these two short datasets, but variations in tundra ecosystem's capacity to emit isoprene (ε in Eq. 6) warrant further study.

The shape of the diurnal cycle of isoprene emissions is similar to the shape observed for mid-latitude ecosystems (compare our Fig. 3 to Fig. 5 in Baldocchi et al., 1995). Night-time emissions are near zero in both cases. Since isoprene emissions require light (cf. Eq. 2), this is the expected result for the mid-latitude ecosystem. Because Toolik is located above the Arctic Circle near 69° N, the sun never set during EC05 or EC10 so this is a less obvious result. But the diurnal cycle in temperature and light were sufficient to suppress night-time isoprene emissions (Figs. 3 and 4). The peak in isoprene emissions occurs around 15:00 LT (Fig. 3) in 2005, which is 1 h after solar noon (14:00 LT) and corresponds to the peak in air temperature. Again, this result is consistent with mid-latitude ecosystems (e.g. Pressley et al., 2005).

3.2.2 Chamber measurements

Static chamber measurements of whole-system isoprene fluxes were performed 6–9 July (day of year 187–190) during 2011. Over these 4 days, 15 samples were collected from 6 different installed bases. Of this set, 4 samples were rejected because the model

BGD
9, 13351–13396, 2012

explained less than 55 % of the variation in isoprene concentration (average r^2 = 0.26). In 2 of these two rejected cases, clouds passed overhead during the measurement and changed PAR values measured inside the enclosure by a factor of 3. Excluding these 4 cases only causes a 5 % increase in the result. For the 11 samples retained, our model explained on average 95 % of the observed variation in isoprene concentrations. The mean of these measurements was 0.45 (SD = 0.19) mg C m^{-2} h^{-1}. Because our static chamber model was based on Eq. (5), this result is effectively EF_{canopy} and can be compared to the EF_{canopy} values calculated for the EC05 and EC11 measurements in Fig. 5. The slope of the line for each year gives EF_{canopy}: 1.93 (EC05) and 0.93 (EC10) mg C m^{-2} h^{-1}. We considered two factors that could explain the differences in emission rates observed between the CH11 and EC05/EC10 measurements: previous temperature and ecosystem composition.

The importance of variability due to previous temperature regime was discussed above for the eddy covariance results. Air temperature data were available from a nearby (less than 1 km) weather station operated by the Environmental Data Team of the Toolik Field Station (http://toolik.alaska.edu/edc/abiotic_monitoring/data_query.php). Over the 4-day sampling period, the 24-h average previous temperature ranged from 9.6 to 14.0 °C, considerably lower than either EC05 (16.8 °C) or EC10 (19.0 °C). Similarly, the 10-day average temperature ranged from 8.7 to 9.4 °C, again lower than the 10.5 and 10.4 °C observed for EC05 and EC10, respectively. The lower values of EF_{canopy} observed for CH11 are consistent with the influence of previous temperatures.

Although the CH11 and EC05/EC10 measurements were both taken from moist acidic tundra ecosystems, there were differences between the sampling locations (Fig. 1). In particular, less *S. pulchra* was present in the ecosystems enclosed by the chambers (CH11). The average percent cover for *S. pulchra* was 1.6 % within the chamber bases (Greg Starr, 2012, personal communication). For the moist acidic tundra ecosystem near the Imnavait Creek flux tower (EC experiments), we estimated an LAI of 0.054 for *S. pulchra* from our transect data, compared to a total LAI of 0.66 from the literature (Williams et al., 2006). This gives a percent coverage of 8.2 %, approximately

BGD
9, 13351–13396, 2012

5 times that observed within the chamber bases for CH11. The impact of this increase in *S. Pulchra* coverage on the predicted canopy emission factor is explored below under the whole-system modelling section.

Isoprene fluxes observed from the smaller dynamic chambers were much lower than observed from the larger static chambers. The data were collected simultaneously (8–9 July, day of year 189–190) and at the same location. No measurements from the dynamic chambers exceeded 0.038 mg C m^{-2} h^{-1}, which was less than 10 % of the values observed from the static chambers. But the smaller dynamic chambers were not representative of the larger moist acidic tundra ecosystem; they were selectively placed over *Sphagnum spp.* (moss). From this, we conclude that the mosses do not contribute significantly (< 10 %) to the entire ecosystem flux of isoprene.

3.3 Whole-system modelling

We tested a very simple model of isoprene emission considering the tundra ecosystem as a "big leaf" (Eq. 5). We were motivated to investigate the use of a big-leaf model because of the relatively short height of plants in the tussock tundra ecosystem and relatively low LAI (LAI = 0.66, Williams et al., 2006). While the model has some predictive capability (solid lines in the 2 left panels of Fig. 5), the model over-predicts at low emission levels and under-predicts at high emission levels, especially in 2005. Results from leaf-level measurements (Fig. 2) demonstrate that these emission algorithms (with parameters derived from temperate species research) perform well for temperature but less satisfactorily for light. Following our results at the leaf-level, we computed a canopy emission factor based on a linear relationship between light and emission rate (using Eq. 4 instead of Eq. 2 for the light relationship, C_L, in Eq. 5). The fraction of variance explained by this modification to the model increased considerably for each year (0.79 to 0.90 for 2005 and 0.68 to 0.79 for 2010).

Although this fit is very good, we were concerned if the model was actually capturing the underlying processes well or if there was covariance between explanatory variables that gave a satisfactory result only valid for our short dataset. Our major concern was

BGD
9, 13351–13396, 2012

the covariance of temperature and light in the datasets and the influence of leaf temperature elevation verses air temperature. Measurements with an infrared thermometer found leaf/ground temperatures reaching up to 10 °C above air temperatures in 2005 (data not shown). The motivation to linearize the light relationship (moving from Eq. 3 to Eq. 4) was based on the leaf-level observations. At the whole-system level linearizing light might give a good fit to the data, but the underlying response at higher light levels could be a combination of two processes. First, isoprene emissions at the leaf-level plateau with increasing light as predicted by Eq. (2). Second, the increasing light levels increase leaf temperature at a constant air temperature. The overall effect would appear to be a linear increase at high light levels. This would be a problem since our big-leaf model uses air temperature, not leaf temperature. To test this concern, we moved to a more sophisticated isoprene emission model which estimates leaf temperatures: MEGAN.

The switch to MEGAN driven by default values from the global database (Guenther et al., 2006) significantly improved the fit versus the big-leaf model (compare left-hand panels of Fig. 5 to left-hand panels of Fig. 6). For the dataset in 2005, the r^2 values increased from 0.79 to 0.86 and in 2010 they increased from 0.68 to 0.74. Interestingly, the results from MEGAN do not explain as much variance as the modified big-leaf model with a linearized light relationship (compare right-hand panels of Fig. 5 to left-hand panels of Fig. 6).

In addition to improving the fit, the MEGAN model also provides an absolute value for the flux to compare to our measured values (Eq. 6). The only adjustment to MEGAN was to use the LAI value with no bare cover. Based on remote sensing data, the grid cell that includes the Toolik area is considered to be 42.5 % bare in the MEGAN database. This is appropriate for the entire cell, but not for the fully vegetated area within the flux tower footprint. For 2005, the fit to default values from MEGAN is surprisingly good: on average, the modelled fluxes are only 18 % higher than the observed fluxes (Fig. 6, top-left panel). As discussed in Sect. 3.2.1, measured whole-system fluxes were higher in 2005 compared with 2010, although environmental conditions were similar. This is

BGD
9, 13351–13396, 2012

also reflected in the comparison of the MEGAN model to the measured fluxes for 2010; the measurements are on average only 40 % of the MEGAN values (Fig. 6, bottom-left panel). Interestingly, some of the highest fluxes measured are much closer to the one-to-one line than lower fluxes.

Again, we explored if this good fit to the global estimate in MEGAN reflected our full understanding of the properties associated with this moist acidic tundra ecosystem. First, the LAI used by MEGAN based on remote sensing data is 1.6. This is much higher than the value typically measured for moist acidic tundra (0.66, Williams et al., 2006) and estimated from a whole-system CO_2 exchange model and measured CO_2 fluxes from the same tower (0.3–0.6, see Fig. 6 in Rastetter et al., 2010). For the second version of the MEGAN model ("localized"; right-hand panels in Fig. 6), we set LAI = 0.66.

The next modification was to use a canopy emission factor (ε in Eq. 6) based on our results from leaf-level and chamber measurements. As a baseline, we used $0.45\,\mathrm{mg\,C\,m^{-2}\,h^{-1}}$ from our chamber measurements. As noted above, there was little *S. pulchra* within the bases used for the chamber measurements: the ground cover of *S. pulchra* was < 1 %. We ascribe the emissions observed from the static chambers to sedge species. We did not conduct an extensive survey of leaf-level emissions from sedge species, but other investigators have found appreciable emissions (Ekberg et al., 2009). Averaging across species (*Eriophorum angustifolium* and *Carex rostrata*), year (2005 and 2006) and season (June through September) for the data reported Ekbert et al. (Table 1, 2009) and then using Eq. (3) to adjust to 30 °C, the average basal emission rate is $4.5\,\mathrm{nmol\,m^{-2}\,s^{-1}}$. This is 36 % of the value we report for *S. pulchra*. To account for the increased abundance of *S. pulchra* at the EC05/10 site, we used the results of our transect survey of *S. pulchra* LAI (0.054). We combined this with our leaf-level emission rate ($12.4\,\mathrm{nmol\,m^{-2}\,s^{-1}}$ for a leaf temperature of 30 °C) from *S. pulchra* to derive a new whole-system emission factor. Using the convention of MEGAN, ε is standardized to an LAI of 5 and is $2.47\,\mathrm{mg\,m^{-2}\,h^{-1}}$ for the combined contribution from sedges and *S. pulchra*. The final modification was to switch the canopy type used by

BGD
9, 13351–13396, 2012

MEGAN, which affects a range of parameters: for example, canopy height, leaf width and reflection and scattering coefficients. The global default in MEGAN for our grid cell is shrub, while grass would be more appropriate for the tundra ecosystem. For example, canopy height is 2 m for shrubs but 0.5 m for grass; the later value is more accurate for the tundra ecosystem.

The results of the MEGAN using localized input values are shown in the right-hand panels of Fig. 6. The amount of variance explained by MEGAN decreases slightly for each year (0.86 to 0.83 for 2005 and 0.74 to 0.72 for 2010) with these changes applied. Note that the change to the canopy emission factor will not affect the fit (variance explained) of the model, so the slight decrease is due to the change in LAI and the change in canopy type from shrub to grass. We are unable to explain why the improvements in the input values to MEGAN did not correspond to an increase in MEGAN's predictive ability, but we note again that the datasets are short and the overall fits are good. The absolute fit is a very good for EC10: the model under predicts measured fluxes by less than 10 %. But conversely, the model under prediction is much worse for EC05; the measured fluxes are a factor of 2.32 higher than predicted by MEGAN. This difference is consistent with our previous discussion of inter-annual effects.

3.4 Atmospheric chemistry modelling

Modelling results demonstrate the impact of the measured isoprene emissions on atmospheric chemistry (Fig. 7). Modelled isoprene concentrations reach almost 1.5 ppb, which is within the range of ambient concentrations observed during our chamber measurements (CH11): 0.64 to 1.61 ppb. In addition, 9 samples of ambient air were collected during the EC10 campaign, with an average value of 1.50 ppb. These measured isoprene concentrations were collected at ground level, so we also compare our modelled results to concentrations observed in the CBL during mission 21 of the ABLE 3A campaign. In a vertical flight profile near Bethel, Alaska over tundra and boreal forest ecosystems, isoprene concentrations ranged between 0.50 and 0.53 ppb below an altitude of 1000 m (see Fig. 17a in Blake et al., 1992). While these observed

BGD
9, 13351–13396, 2012

concentrations are lower than modelled, the strength of isoprene emissions in the flight source region is unknown. The sharp decrease in isoprene concentrations with height above 1000 m altitude supports our selection of that value for the CBL height. Observed ozone concentrations (30 to 31 ppb) during the same flight at the same altitudes are consistent with our initialization value (32 ppb).

With the inclusion of the isoprene source, the model predicts a greater than 50 % reduction in the maximum hydroxyl radical (HO) concentration and even greater reductions past solar noon (14:00 local time). The loss rate of ozone increases with the addition of the isoprene source because of the direct reaction of ozone with the double carbon-carbon bonds in isoprene. This is in contrast to the situation over most of the contiguous United States, where isoprene emissions contribute to ozone formation (Chameides et al., 1988). The reason is the relatively low NO_x ($NO_x = NO + NO_2$) concentrations used in the model. Overall, these results demonstrate that the observed isoprene fluxes have a significant impact on atmospheric chemistry.

4 Conclusions

4.1 Global isoprene models

In order to test our hypotheses, we first needed to understand if current models of isoprene emission are adequate for tundra ecosystems and plant species. Our results lend support to the hypothesis of Arneth et al. (2008). Arneth et al. start with the observation that different groups modelling global isoprene emissions often converge on the same estimate (Table 1, Arneth et al., 2008). But they find this convergence "is in stark contrast with our lack of process understanding and the small number of observations for model parameterisation and evaluation" (abstract, Arneth et al., 2008). While our measured whole-system fluxes are in reasonable agreement with predictions from global models, this agreement was based on offsetting errors in two important parameters. First, the actual LAI of the ecosystem was lower than predicted by MEGAN (0.66

BGD
9, 13351–13396, 2012

compared to 1.6). Second, the actual canopy emission factor was higher than predicted (3.74 compared to 2.47 $mg\,m^{-2}\,h^{-1}$). While these errors offset each other to produce an overall modelled estimate that was close to our observations, this is only a fortuitous result. More generally, errors such as these demonstrate that much more experimental data are necessary to improve the parameters used by these models. Moving past improved parameterization and more to the point of Arneth et al., there are indications that the underlying algorithms used in MEGAN are not optimal for the tundra ecosystem. A far simpler model that uses only air temperature and light had a better fit than the comparatively complicated global model. This simple model was based on the standard Guenther algorithm for temperature, but used a linear relationship for light. Much longer datasets of whole-system emissions from a variety of ecosystem types need to be collected to fully understand the relevance of this observation.

4.2 Arctic atmospheric chemistry

The reduction in OH concentrations predicted by RACM has a significant impact on the chemical loss rate of a reactive hydrocarbon found in the Arctic due to long-range transport: benzene (C_6H_6). The maximum chemical loss rate due to the reaction of benzene with OH decreases with the addition of isoprene by just over a factor of two (2.02, Fig. 7), which is equivalent to a doubling of chemical lifetime of benzene. Benzene is a reasonable surrogate for other hydrocarbons in the Arctic atmosphere. In particular, the chemical loss rates of persistent organic pollutants (POPs) are important for understanding their transport and fate in the Artic. Currently, investigators have hypothesized that Arctic warming is leading to remobilization of these POPs (Ma et al., 2011). We speculate if remobilization continues to occur, redeposition of these POPs will increase in the Arctic because of the decrease in chemical oxidation. To fully predict future transport of these remobilized POPs, changes in chemical loss rates due to potential changes in isoprene emission rates should be considered.

BGD
9, 13351–13396, 2012

4.3 Global climate change and future emissions from Arctic ecosystems

Based on our results, we predict that isoprene emissions from Arctic ecosystems will increase due to future climate change. Predicting future isoprene emissions from any ecosystem is a two-step process. First, the factors that control isoprene emissions must be identified and their relationship to emissions understood. Second, predictions of how the identified factors will change in the future are necessary. Temperature is the one factor that is relatively straightforward. A simple extrapolation using the Guenther algorithm (Eq. 3) and the predicted rise in global temperature over the next century (2 to 3 °C) gives an increase of 30 to 45 % in predicted global isoprene emissions (Peñuelas and Llusià, 2003). For the Arctic, the temperature increase is expected to be greater than the global increase (IPCC, 2007), which should lead increases in BVOC emissions that are similarly larger than those predicted for the rest of the Earth. This prediction is supported by our observation that the simulated warming experiment increased isoprene emission rates by a factor of 3. But this only considers the direct effect of temperature. The response of isoprene emission to other global change factors (CO_2 concentration, nutrient addition, UV radiation, ozone, and water stress) is more complicated, with isoprene emissions responding differently in different experiments (Penuelas and Staudt, 2010). For example, one global change factor, fertilization by nitrogen and phosphorous, had no impact on leaf-level isoprene emissions in our experiment.

Further, changes in ecosystem species composition due to changing climate could cause major shifts in the canopy emission factor (ε). Increasing temperatures have caused an increase in woody shrubs in areas that are currently tundra ecosystems (Elmendorf et al., 2012). If this leads to increases in the abundance of *Salix* or other isoprene-emitting genera, then there will be increases in ε. But if non-emitting genera like *Betula* (birch) increase, then ε could decrease. This was observed in a warming experiment near the Toolik Field Station (Hobbie and Chapin, 1998), where the aboveground biomass of *Betula nana* increased almost two fold. We note that *Salix*

BGD
9, 13351–13396, 2012

was relatively rare at this experimental location. But another recent study found specifically that *Salix* growth would be favoured in the north-western Eurasian tundra due to teleconnections between atmospheric circulation and air-surface exchanges (Macias-Fauria et al., 2012). Our overall conclusion is that predicting future isoprene emissions from tundra ecosystems will rely both on a better understanding of the processes that control emissions from these high-latitude ecosystems and detailed predictions of future ecosystem future and composition. Given the uncertainty, we do predict that temperature will be the dominate factor, and that isoprene emissions from tundra ecosystems could become comparable to mid-latitude ecosystems.

Acknowledgements. The authors (MJP and BMB) gratefully acknowledge support from the National Science Foundation for a Collaborative Research award entitled Biogenic Volatile Organic Compound Emissions from the Tundra and Arctic Atmospheric Chemistry (1025948). This work was also supported by project numbers 0221835 (Biocomplexity) and 0732664 (IPY) from the National Science Foundation to KLG. We also thank Gus Shaver and John Hobbie from the Marine Biological Laboratory for advice, logistical support and access to the global change plots. Finally, we very much appreciate the logistical support we received from Chad Diesinger and the staff at the Toolik Field Station and Institute for Arctic Biology at the University of Alaska-Fairbanks.

References

Andreae, M. O. and Crutzen, P. J.: Atmospheric aerosols: biogeochemical sources and role in atmospheric chemistry, Science, 276, 1052–1058, 1997.

Arneth, A., Monson, R. K., Schurgers, G., Niinemets, Ü., and Palmer, P. I.: Why are estimates of global terrestrial isoprene emissions so similar (and why is this not so for monoterpenes)?, Atmos. Chem. Phys., 8, 4605–4620, doi:10.5194/acp-8-4605-2008, 2008.

Aubinet, M., Grelle, A., Ibrom, A., Rannik, U., Moncrieff, J., Foken, T., Kowalski, A. S., Martin, P. H., Berbigier, P., Bernhofer, C., Clement, R., Elbers, J., Granier, A., Grunwald, T., Morgenstern, K., Pilegaard, K., Rebmann, C., Snijders, W., Valentini, R., and Vesala, T.: Estimates of the annual net carbon and water exchange of forests: the EUROFLUX methodology, Adv. Ecol. Res., 30, 113–175, 2000.

BGD
9, 13351–13396, 2012

Bakwin, P. S., Wofsy, S. C., Fan, S. M., and Fitzjarrald, D. R.: Measurements of NO_x and NO_y concentrations and fluxes over Arctic Tundra, J. Geophys. Res.-Atmos., 97, 16545–16557, 1992.

Baldocchi, D. D.: Assessing the eddy covariance technique for evaluating carbon dioxide exchange rates of ecosystems: past, present and future, Glob. Change Biol., 9, 479–492, 2003.

Baldocchi, D., Guenther, A., Harley, P., Klinger, L., Zimmerman, P., Lamb, B., and Westberg, H.: The fluxes and air chemistry of isoprene above a deciduous hardwood forest, Philos. T. Roy. Soc. A, 351, 279–296, 1995.

Baldocchi, D. D., Fuentes, J. D., Bowling, D. R., Turnipseed, A. A., and Monson, R. K.: Scaling isoprene fluxes from leaves to canopies: test cases over a boreal aspen and a mixed species temperate forest, J. Appl. Meteorol., 38, 885–898, 1999.

Baldocchi, D., Falge, E., Gu, L. H., Olson, R., Hollinger, D., Running, S., Anthoni, P., Bernhofer, C., Davis, K., Evans, R., Fuentes, J., Goldstein, A., Katul, G., Law, B., Lee, X. H., Malhi, Y., Meyers, T., Munger, W., Oechel, W., Paw U, K. T., Pilegaard, K., Schmid, H. P., Valentini, R., Verma, S., Vesala, T., Wilson, K., and Wofsy, S.: FLUXNET: A new tool to study the temporal and spatial variability of ecosystem-scale carbon dioxide, water vapor, and energy flux densities, B. Am. Meteorol. Soc., 82, 2415–2434, 2001.

Barrie, L. A., Bottenheim, J. W., Schnell, R. C., Crutzen, P. J., and Rasmussen, R. A.: Ozone destruction and photochemical-reactions at polar sunrise in the lower arctic atmosphere, Nature, 334, 138–141, 1988.

Bartlett, K. B., Crill, P. M., Sass, R. L., Harriss, R. C., and Dise, N. B.: Methane emissions from tundra environments in the Yukon-Kuskokwim Delta, Alaska, J. Geophys. Res.-Atmos., 97, 16645–16660, 1992.

Blake, D. R., Hurst, D. F., Smith, T. W., Whipple, W. J., Chen, T. Y., Blake, N. J., and Rowland, F. S.: Summertime measurements of selected nonmethane hydrocarbons in the Arctic and Sub-Arctic during the 1988 Arctic Boundary-Layer Expedition (ABLE-3A), J. Geophys. Res.-Atmos., 97, 16559–16588, 1992.

Boelman, N. T., Gough, L., McLaren, J. R., and Greaves, H.: Does NDVI reflect variation in the structural attributes associated with increasing shrub dominance in arctic tundra?, Environ. Res. Lett., 6, 035501, doi:10.1088/1748-9326/6/3/035501, 2011.

Bret-Harte, M. S., Shaver, G. R., Zoerner, J. P., Johnstone, J. F., Wagner, J. L., Chavez, A. S., Gunkelman, R. F., Lippert, S. C., and Laundre, J. A.: Developmental plasticity allows Betula nana to dominate tundra subjected to an altered environment, Ecology, 82, 18–32, 2001.

BGD
9, 13351–13396, 2012

Chameides, W. L., Lindsay, R. W., Richardson, J., and Kiang, C. S.: The role of biogenic hydrocarbons in urban photochemical smog – Atlanta as a case-study, Science, 241, 1473–1475, 1988.
Chapin, F. S., Shaver, G. R., Giblin, A. E., Nadelhoffer, K. J., and Laundre, J. A.: Responses of Arctic Tundra to experimental and observed changes in climate, Ecology, 76, 694–711, 1995.
Chen, W. J., Zhang, Y., Cihlar, J., Smith, S. L., and Riseborough, D. W.: Changes in soil temperature and active layer thickness during the twentieth century in a region in Western Canada, J. Geophys. Res.-Atmos., 108, 4696, doi:10.1029/2002jd003355, 2003.
Clark, P. U., Pisias, N. G., Stocker, T. F., and Weaver, A. J.: The role of the thermohaline circulation in abrupt climate change, Nature, 415, 863–869, 2002.
Comiso, J. C. and Parkinson, C. L.: Satellite-observed changes in the Arctic, Phys. Today, 57, 38–44, 2004.
Crutzen, P. J. and Zimmermann, P. H.: The changing photochemistry of the troposphere, Tellus A, 43, 136–151, 1991.
Ekberg, A., Arneth, A., Hakola, H., Hayward, S., and Holst, T.: Isoprene emission from wetland sedges, Biogeosciences, 6, 601–613, doi:10.5194/bg-6-601-2009, 2009.
Elmendorf, S. C., Henry, G. H. R., Hollister, R. D., Bjork, R. G., Boulanger-Lapointe, N., Cooper, E. J., Cornelissen, J. H. C., Day, T. A., Dorrepaal, E., Elumeeva, T. G., Gill, M., Gould, W. A., Harte, J., Hik, D. S., Hofgaard, A., Johnson, D. R., Johnstone, J. F., Jonsdottir, I. S., Jorgenson, J. C., Klanderud, K., Klein, J. A., Koh, S., Kudo, G., Lara, M., Levesque, E., Magnusson, B., May, J. L., Mercado-Diaz, J. A., Michelsen, A., Molau, U., Myers-Smith, I. H., Oberbauer, S. F., Onipchenko, V. G., Rixen, C., Martin Schmidt, N., Shaver, G. R., Spasojevic, M. J., Orhallsdottir, O. E., Tolvanen, A., Troxler, T., Tweedie, C. E., Villareal, S., Wahren, C.-H., Walker, X., Webber, P. J., Welker, J. M., and Wipf, S.: Plot-scale evidence of tundra vegetation change and links to recent summer warming, Nature Clim. Change, 2, 453–457, available at: http://www.nature.com/nclimate/journal/v2/n6/abs/nclimate1465.html#supplementary-information, 2012.
Euskirchen, E. S., Bret-Harte, M. S., Scott, G. J., Edgar, C., and Shaver, G. R.: Seasonal patterns of carbon dioxide and water fluxes in three representative tundra ecosystems in Northern Alaska, Ecosphere, 3, 4, doi:10.1890/es11-00202.1, 2012.
Fall, R.: Abundant oxygenates in the atmosphere: a biochemical perspective, Chem. Rev., 103, 4941–4951, doi:10.1021/Cr0206521, 2003.

BGD
9, 13351–13396, 2012

Faubert, P., Tiiva, P., Rinnan, A., Michelsen, A., Holopainen, J. K., and Rinnan, R.: Doubled volatile organic compound emissions from subarctic tundra under simulated climate warming, New Phytol., 187, 199–208, doi:10.1111/j.1469-8137.2010.03270.x, 2010.
Forbes, B. C., Fauria, M. M., and Zetterberg, P.: Russian Arctic warming and "greening" are closely tracked by tundra shrub willows, Glob. Change Biol., 16, 1542–1554, doi:10.1111/j.1365-2486.2009.02047.x, 2010.
Frauenfeld, O. W., Zhang, T. J., Barry, R. G., and Gilichinsky, D.: Interdecadal changes in seasonal freeze and thaw depths in Russia, J. Geophys. Res.-Atmos., 109, D05101, doi:10.1029/2003jd004245, 2004.
Geron, C., Guenther, A., Greenberg, J., Loescher, H. W., Clark, D., and Baker, B.: Biogenic volatile organic compound emissions from a lowland tropical wet forest in Costa Rica, Atmos. Environ., 36, 3793–3802, 2002.
Goldstein, A. H., Daube, B. C., Munger, J. W., and Wofsy, S. C.: Automated in-situ monitoring of atmospheric nonmethane hydrocarbon concentrations and gradients, J. Atmos. Chem., 21, 43–59, 1995.
Gough, L., and Hobbie, S. E.: Responses of moist non-acidic arctic tundra to altered environment: productivity, biomass, and species richness, Oikos, 103, 204–216, 2003.
Goulden, M. L., Munger, J. W., Fan, S.-M., Daube, B. C., and Wofsy, S. C.: Measurements of carbon sequestration by long-term eddy covariance: methods and a critical evaluation of accuracy, Glob. Change Biol., 2, 169–182, doi:10.1111/j.1365-2486.1996.tb00070.x, 1996.
Gregory, G. L., Anderson, B. E., Warren, L. S., Browell, E. V., Bagwell, D. R., and Hudgins, C. H.: Tropospheric ozone and aerosol observations: the Alaskan Arctic, J. Geophys. Res., 97, 16451–16471, doi:10.1029/91jd01310, 1992.
Guenther, A. B. and Hills, A. J.: Eddy covariance measurement of isoprene fluxes, J. Geophys. Res.-Atmos., 103, 13145–13152, 1998.
Guenther, A. B., Zimmerman, P. R., Harley, P. C., Monson, R. K., and Fall, R.: Isoprene and monoterpene emission rate variability – model evaluations and sensitivity analyses, J. Geophys. Res.-Atmos., 98, 12609–12617, 1993.
Guenther, A., Otter, L., Zimmerman, P., Greenberg, J., Scholes, R., and Scholes, M.: Biogenic hydrocarbon emissions from Southern African savannas, J. Geophys. Res.-Atmos., 101, 25859–25865, 1996.
Guenther, A., Karl, T., Harley, P., Wiedinmyer, C., Palmer, P. I., and Geron, C.: Estimates of global terrestrial isoprene emissions using MEGAN (Model of Emissions of Gases and

BGD
9, 13351–13396, 2012

Aerosols from Nature), Atmos. Chem. Phys., 6, 3181–3210, doi:10.5194/acp-6-3181-2006, 2006.
Harley, P. C., Litvak, M. E., Sharkey, T. D., and Monson, R. K.: Isoprene emission from velvet bean-leaves – interactions among nitrogen availability, growth photon flux-density, and leaf development, Plant Physiol., 105, 279–285, 1994.
Harley, P., Guenther, A., and Zimmerman, P.: Effects of light, temperature and canopy position on net photosynthesis and isoprene emission from sweetgum (*Liquidambar styraciflua*) leaves, Tree Physiol., 16, 25–32, 1996.
Harriss, R. C., Sachse, G. W., Hill, G. F., Wade, L., Bartlett, K. B., Collins, J. E., Steele, L. P., and Novelli, P. C.: Carbon monoxide and methane in the North American arctic and subarctic troposphere: July–August 1988, J. Geophys. Res., 97, 16589–16599, doi:10.1029/91jd02037, 1992a.
Harriss, R. C., Wofsy, S. C., Bartlett, D. S., Shipham, M. C., Jacob, D. J., Hoell, J. M., Bendura, R. J., Drewry, J. W., Mcneal, R. J., Navarro, R. L., Gidge, R. N., and Rabine, V. E.: The Arctic Boundary-Layer Expedition (ABLE-3A) – July–August 1988, J. Geophys. Res.-Atmos., 97, 16383–16394, 1992b.
Helmig, D., Oltmans, S. J., Carlson, D., Lamarque, J. F., Jones, A., Labuschagne, C., Anlauf, K., and Hayden, K.: A review of surface ozone in the polar regions, Atmos. Environ., 41, 5138–5161, doi:10.1016/j.atmosenv.2006.09.053, 2007.
Hobbie, S. E. and Chapin, F. S.: Response of tundra plant biomass, aboveground production, nitrogen, and CO_2 flux to experimental warming, Ecology, 79, 1526–1544, 1998.
IPCC: Climate Change 2007 – The Physical Science Basis: Working Group I Contribution to the Fourth Assessment Report of the IPCC, edited by: Solomon, S., Qin, D., Manning, M., Chen, Z., Marquis, M., Averyt, K. B., Tignor, M., and Miller, H. L., Cambridge University Press, Cambridge, 2007.
Jacob, D. J., Fan, S. M., Wofsy, S. C., Spiro, P. A., Bakwin, P. S., Ritter, J. A., Browell, E. V., Gregory, G. L., Fitzjarrald, D. R., and Moore, K. E.: Deposition of ozone to tundra, J. Geophys. Res.-Atmos., 97, 16473–16479, 1992.
Karl, T., Potosnak, M., Guenther, A., Clark, D., Walker, J., Herrick, J. D., and Geron, C.: Exchange processes of volatile organic compounds above a tropical rain forest: implications for modeling tropospheric chemistry above dense vegetation, J. Geophys. Res.-Atmos., 109, D18306, doi:10.1029/2004jd004738, 2004.

BGD
9, 13351–13396, 2012

Keller, M. and Lerdau, M.: Isoprene emission from tropical forest canopy leaves, Global Biogeochem. Cy., 13, 19–29, 1999.
Kwok, R., Cunningham, G. F., Wensnahan, M., Rigor, I., Zwally, H. J., and Yi, D.: Thinning and volume loss of the Arctic Ocean sea ice cover: 2003–2008, J. Geophys. Res.-Oceans, 114, C07005, doi:10.1029/2009jc005312, 2009.
Langford, B., Misztal, P. K., Nemitz, E., Davison, B., Helfter, C., Pugh, T. A. M., MacKenzie, A. R., Lim, S. F., and Hewitt, C. N.: Fluxes and concentrations of volatile organic compounds from a South-East Asian tropical rainforest, Atmos. Chem. Phys., 10, 8391–8412, doi:10.5194/acp-10-8391-2010, 2010.
Lathiere, J., Hewitt, C. N., and Beerling, D. J.: Sensitivity of isoprene emissions from the terrestrial biosphere to 20th century changes in atmospheric CO_2 concentration, climate, and land use, Global Biogeochem. Cy., 24, GB1004, doi:10.1029/2009gb003548, 2010.
Liberto, L. D., Angelini, F., Pietroni, I., Cairo, F., Donfrancesco, G. D., Viola, A., Argentini, S., Fierli, F., Gobbi, G., Maturilli, M., Neuber, R., and Snels, M.: Estimate of the arctic convective boundary layer height from lidar observations: a case study, Adv. Meteorol., 9, 851927, doi:10.1155/2012/851927, 2012.
Loreto, F., Mannozzi, M., Maris, C., Nascetti, P., Ferranti, F., and Pasqualini, S.: Ozone quenching properties of isoprene and its antioxidant role in leaves, Plant Physiol., 126, 993–1000, 2001.
Ma, J., Hung, H., Tian, C., and Kallenborn, R.: Revolatilization of persistent organic pollutants in the Arctic induced by climate change, Nature Clim. Change, 1, 255–260, 2011.
Macias-Fauria, M., Forbes, B. C., Zetterberg, P., and Kumpula, T.: Eurasian Arctic greening reveals teleconnections and the potential for structurally novel ecosystems, Nature Clim. Change, available at: http://www.nature.com/nclimate/journal/v2/n8/abs/nclimate1558.html#supplementary-information, 2012.
McKinney, K. A., Lee, B. H., Vasta, A., Pho, T. V., and Munger, J. W.: Emissions of isoprenoids and oxygenated biogenic volatile organic compounds from a New England mixed forest, Atmos. Chem. Phys., 11, 4807–4831, doi:10.5194/acp-11-4807-2011, 2011.
Monson, R. K. and Fall, R.: Isoprene emission from aspen leaves – influence of environment and relation to photosynthesis and photorespiration, Plant Physiol., 90, 267–274, 1989.
Myneni, R. B., Keeling, C. D., Tucker, C. J., Asrar, G., and Nemani, R. R.: Increased plant growth in the northern high latitudes from 1981 to 1991, Nature, 386, 698–702, 1997.

BGD
9, 13351–13396, 2012

Nay, S. M., Mattson, K. G., and Bormann, B. T.: Biases of chamber methods for measuring soil CO_2 efflux demonstrated with a laboratory apparatus, Ecology, 75, 2460–2463, 1994.
Ortega, J. and Helmig, D.: Approaches for quantifying reactive and low-volatility biogenic organic compound emissions by vegetation enclosure techniques – Part A, Chemosphere, 72, 343–364, doi:10.1016/j.chemosphere.2007.11.020, 2008.
Otter, L., Guenther, A., Wiedinmyer, C., Fleming, G., Harley, P., and Greenberg, J.: Spatial and temporal variations in biogenic volatile organic compound emissions for Africa south of the equator, J. Geophys. Res.-Atmos., 108, 8505, doi:10.1029/2002jd002609, 2003.
Overpeck, J., Hughen, K., Hardy, D., Bradley, R., Case, R., Douglas, M., Finney, B., Gajewski, K., Jacoby, G., Jennings, A., Lamoureux, S., Lasca, A., MacDonald, G., Moore, J., Retelle, M., Smith, S., Wolfe, A., and Zielinski, G.: Arctic environmental change of the last four centuries, Science, 278, 1251–1256, 1997.
Papiez, M. R., Potosnak, M. J., Goliff, W. S., Guenther, A. B., Matsunaga, S. N., and Stockwell, W. R.: The impacts of reactive terpene emissions from plants on air quality in Las Vegas, Nevada, Atmos. Environ., 43, 4109–4123, doi:10.1016/j.atmosenv.2009.05.048, 2009.
Peñuelas, J. and Llusià, J.: BVOCs: plant defense against climate warming?, Trends Plant Sci., 8, 105–109, doi:10.1016/s1360-1385(03)00008-6, 2003.
Peñuelas, J. and Staudt, M.: BVOCs and global change, Trends Plant Sci., 15, 133–144, doi:10.1016/j.tplants.2009.12.005, 2010.
Petron, G., Harley, P., Greenberg, J., and Guenther, A.: Seasonal temperature variations influence isoprene emission, Geophys. Res. Lett., 28, 1707–1710, 2001.
Pressley, S., Lamb, B., Westberg, H., Flaherty, J., Chen, J., and Vogel, C.: Long-term isoprene flux measurements above a northern hardwood forest, J. Geophys. Res.-Atmos., 110, D07301, doi:10.1029/2004jd005523, 2005.
Rasmussen, R. A. and Khalil, M. A. K.: Atmospheric benzene and toluene, Geophys. Res. Lett., 10, 1096–1099, doi:10.1029/GL010i011p01096, 1983.
Rastetter, E. B., Williams, M., Griffin, K. L., Kwiatkowski, B. L., Tomasky, G., Potosnak, M. J., Stoy, P. C., Shaver, G. R., Stieglitz, M., Hobbie, J. E., and Kling, G. W.: Processing arctic eddy-flux data using a simple carbon-exchange model embedded in the ensemble Kalman filter, Ecol. Appl., 20, 1285–1301, 2010.
Rawlins, M. A., Steele, M., Holland, M. M., Adam, J. C., Cherry, J. E., Francis, J. A., Groisman, P. Y., Hinzman, L. D., Huntington, T. G., Kane, D. L., Kimball, J. S., Kwok, R., Lammers, R. B., Lee, C. M., Lettenmaier, D. P., McDonald, K. C., Podest, E., Pundsack, J. W., Rudels, B.,

BGD
9, 13351–13396, 2012

and Serreze, M. C.: Analysis of the Arctic System for Freshwater Cycle Intensification: Observations and Expectations, J. Climate, 23, 5715–5737, doi:10.1175/2010jcli3421.1, 2010.
Rinnan, R., Rinnan, A., Faubert, P., Tiiva, P., Holopainen, J. K., and Michelsen, A.: Few long-term effects of simulated climate change on volatile organic compound emissions and leaf chemistry of three subarctic dwarf shrubs, Environ. Exp. Bot., 72, 377–386, doi:10.1016/j.envexpbot.2010.11.006, 2011.
Rinne, H. J. I., Guenther, A. B., Greenberg, J. P., and Harley, P. C.: Isoprene and monoterpene fluxes measured above Amazonian rainforest and their dependence on light and temperature, Atmos. Environ., 36, 2421–2426, 2002.
Rinne, J., Hakola, H., Laurila, T., and Rannik, U.: Canopy scale monoterpene emissions of Pinus sylvestris dominated forests, Atmos. Environ., 34, 1099–1107, 2000.
Rosenstiel, T. N., Ebbets, A. L., Khatri, W. C., Fall, R., and Monson, R. K.: Induction of poplar leaf nitrate reductase: a test of extrachloroplastic control of isoprene emission rate, Plant Biol., 6, 12–21, doi:10.1055/S-2003-44722, 2004.
Sandholm, S. T., Bradshaw, J. D., Chen, G., Singh, H. B., Talbot, R. W., Gregory, G. L., Blake, D. R., Sachse, G. W., Browell, E. V., Barrick, J. D. W., Shipham, M. A., Bachmeier, A. S., and Owen, D.: Summertime tropospheric observations related to N_xO_y distributions and partitioning over Alaska: Arctic Boundary Layer Expedition 3A, J. Geophys. Res., 97, 16481–16509, doi:10.1029/92jd01491, 1992.
Serreze, M. C., Walsh, J. E., Chapin, F. S., Osterkamp, T., Dyurgerov, M., Romanovsky, V., Oechel, W. C., Morison, J., Zhang, T., and Barry, R. G.: Observational evidence of recent change in the northern high-latitude environment, Climat. Change, 46, 159–207, 2000.
Sharkey, T. D. and Singsaas, E. L.: Why plants emit isoprene, Nature, 374, 769–769, 1995.
Sharkey, T. D. and Yeh, S. S.: Isoprene emission from plants, Annu. Rev. Plant Phys., 52, 407–436, 2001.
Sharkey, T. D., Singsaas, E. L., Lerdau, M. T., and Geron, C. D.: Weather effects on isoprene emission capacity and applications in emissions algorithms, Ecol. Appl., 9, 1132–1137, 1999.
Shaver, G. R., Bret-Harte, S. M., Jones, M. H., Johnstone, J., Gough, L., Laundre, J., and Chapin, F. S.: Species composition interacts with fertilizer to control long-term change in tundra productivity, Ecology, 82, 3163–3181, 2001.
Singh, H. B., O'Hara, D., Herlth, D., Bradshaw, J. D., Sandholm, S. T., Gregory, G. L., Sachse, G. W., Blake, D. R., Crutzen, P. J., and Kanakidou, M. A.: Atmospheric Measure-

BGD
9, 13351–13396, 2012

ments of peroxyacetyl nitrate and other organic nitrates at high latitudes: possible sources and sinks, J. Geophys. Res., 97, 16511–16522, doi:10.1029/91jd00889, 1992.
Spirig, C., Guenther, A., Greenberg, J. P., Calanca, P., and Tarvainen, V.: Tethered balloon measurements of biogenic volatile organic compounds at a Boreal forest site, Atmos. Chem. Phys., 4, 215–229, doi:10.5194/acp-4-215-2004, 2004.
Stockwell, W. R. and Goliff, W. S.: Measurement of actinic flux and the calculation of photolysis rate parameters for the Central California Ozone Study, Atmos. Environ., 38, 5169–5177, doi:10.1016/j.atmosenv.2004.05.048, 2004.
Sturm, M., McFadden, J. P., Liston, G. E., Chapin, F. S., Racine, C. H., and Holmgren, J.: Snow-shrub interactions in Arctic tundra: a hypothesis with climatic implications, J. Climate, 14, 336–344, 2001.
Sumner, A. L. and Shepson, P. B.: Snowpack production of formaldehyde and its effect on the Arctic troposphere, Nature, 398, 230–233, 1999.
Sumner, A. L., Shepson, P. B., Grannas, A. M., Bottenheim, J. W., Anlauf, K. G., Worthy, D., Schroeder, W. H., Steffen, A., Domine, F., Perrier, S., and Houdier, S.: Atmospheric chemistry of formaldehyde in the Arctic troposphere at Polar Sunrise, and the influence of the snowpack, Atmos. Environ., 36, 2553–2562, 2002.
Talbot, R. W., Vijgen, A. S., and Harriss, R. C.: Soluble species in the Arctic summer troposphere: acidic gases, aerosols, and precipitation, J. Geophys. Res., 97, 16531–16543, doi:10.1029/91jd00118, 1992.
Tape, K., Sturm, M., and Racine, C.: The evidence for shrub expansion in Northern Alaska and the Pan-Arctic, Glob. Change Biol., 12, 686–702, doi:10.1111/j.1365-2486.2006.01128.x, 2006.
Tiiva, P., Rinnan, R., Faubert, P., Rasanen, J., Holopainen, T., Kyro, E., and Holopainen, J. K.: Isoprene emission from a subarctic peatland under enhanced UV-B radiation, New Phytol., 176, 346–355, doi:10.1111/j.1469-8137.2007.02164.x, 2007.
Tiiva, P., Faubert, P., Michelsen, A., Holopainen, T., Holopainen, J. K., and Rinnan, R.: Climatic warming increases isoprene emission from a subarctic heath, New Phytol., 180, 853–863, doi:10.1111/j.1469-8137.2008.02587.x, 2008.
Trapp, S. and Croteau, R.: Defensive resin biosynthesis in conifers, Annu. Rev. Plant Phys., 52, 689–724, 2001.

BGD
9, 13351–13396, 2012

Turnipseed, A. A., Anderson, D. E., Blanken, P. D., Baugh, W. M., and Monson, R. K.: Airflows and turbulent flux measurements in mountainous terrain Part 1. Canopy and local effects, Agr. Forest Meteorol., 119, 1–21, doi:10.1016/S0168-1923(03)00136-9, 2003.

van Wijk, M. T., Clemmensen, K. E., Shaver, G. R., Williams, M., Callaghan, T. V., Chapin, F. S., Cornelissen, J. H. C., Gough, L., Hobbie, S. E., Jonasson, S., Lee, J. A., Michelsen, A., Press, M. C., Richardson, S. J., and Rueth, H.: Long-term ecosystem level experiments at Toolik Lake, Alaska, and at Abisko, Northern Sweden: generalizations and differences in ecosystem and plant type responses to global change, Glob. Change Biol., 10, 105–123, 2004.

Walker, M. D., Walker, D. A., Welker, J. M., Arft, A. M., Bardsley, T., Brooks, P. D., Fahnestock, J. T., Jones, M. H., Losleben, M., Parsons, A. N., Seastedt, T. R., and Turner, P. L.: Long-term experimental manipulation of winter snow regime and summer temperature in arctic and alpine tundra, Hydrol. Process., 13, 2315–2330, 1999.

Webb, E. K., Pearman, G. I., and Leuning, R.: Correction of flux measurements for density effects due to heat and water vapour transfer, Quarterly J. Roy. Meteorol. Soc., 106, 85–100, doi:10.1002/qj.49710644707, 1980.

Wiedinmyer, C., Guenther, A., Harley, P., Hewitt, C. N., Geron, C., Artaxo, P., Steinbrecher, R., Rasmussen: global organic emissions from vegetation, in: Emissions Of Atmospheric Trace Compounds, edited by: Granier, C., Artaxo, P. E., and Reeves, C. E., Kluwer Academic Publishers, Dordrecht, The Netherlands, 115–170, 2004.

Wilczak, J. M., Oncley, S. P., and Stage, S. A.: Sonic anemometer tilt correction algorithms, Bound.-Lay. Meteorol., 99, 127–150, 2001.

Williams, M., Street, L. E., van Wijk, M. T., and Shaver, G. R.: Identifying differences in carbon exchange among arctic ecosystem types, Ecosystems, 9, 288–304, doi:10.1007/s10021-005-0146-y, 2006.

BGD
9, 13351–13396, 2012

Table 1. Concentrations and sources used to initialize the RACM model. PAN is peroxyacyl nitrates.

Species	Concentration	Units	Source
O_3	32	ppb	Gregory et al. (1992)
NO	8.5	ppt	Sandholm et al. (1992)
NO_2	16.5	ppt	Sandholm et al. (1992)
HNO_3	40	ppt	Talbot et al. (1992)
PAN	25	ppt	Singh et al. (1992)
CO	90	ppb	Harriss et al. (1992a)
CH_4	1.73	ppm	Harriss et al. (1992a)
Ethyne	40	ppt	Blake et al. (1992)
Toluene	47	ppt	Rasmussen and Khalil (1983)
Benzene	167	ppt	Rasmussen and Khalil (1983)

BGD
9, 13351–13396, 2012

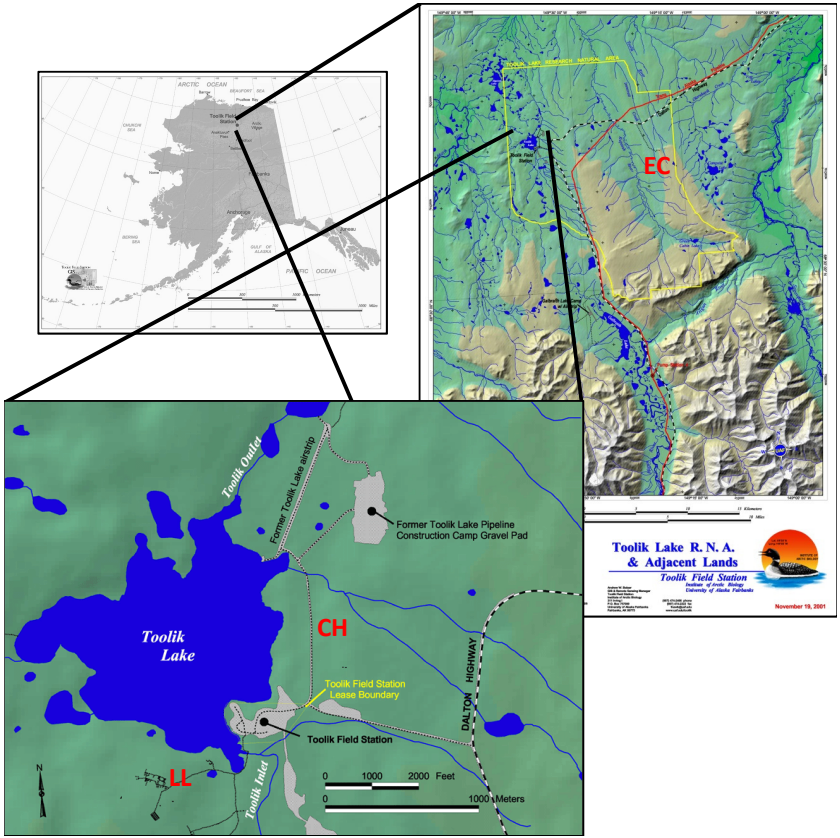

Fig. 1. The Toolik Field Station is located on the north slope of the Brooks Range. The Imnavait Creek experimental watershed (marked EC) is 12 km east of the main field station, and is at an elevation of 930 m. The chamber measurements were located just north of the field station (marked CH). Leaf-level measurements were performed to the southwest of the station (marked LL). (Map courtesy of the Toolik Field Station GIS Office, http://toolik.alaska.edu/gis/maps/index.php).

BGD
9, 13351–13396, 2012

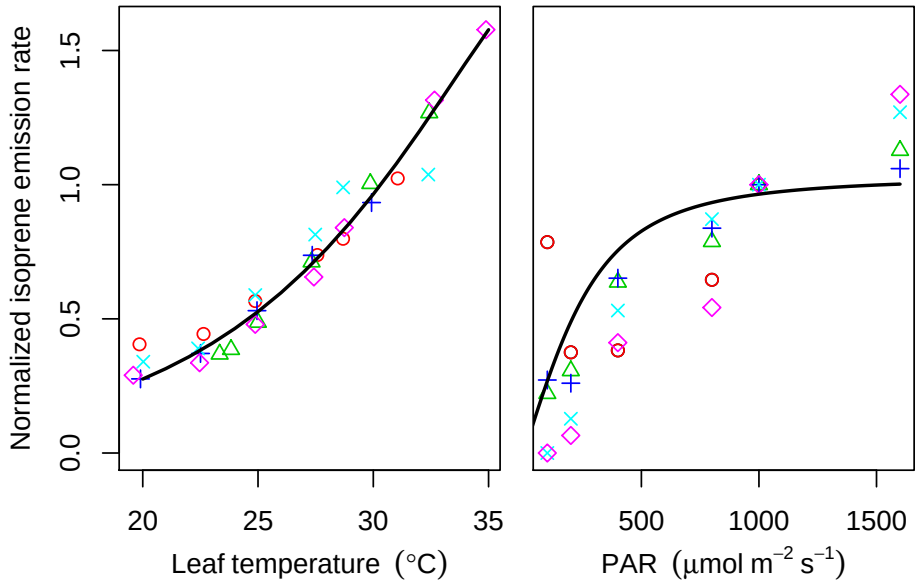

Fig. 2. Normalized isoprene emissions as a function of leaf temperature and light compared to the G93 algorithm (black curves). The individual sets of measurements are denoted by the same colour and type of plotting character.

BGD
9, 13351–13396, 2012

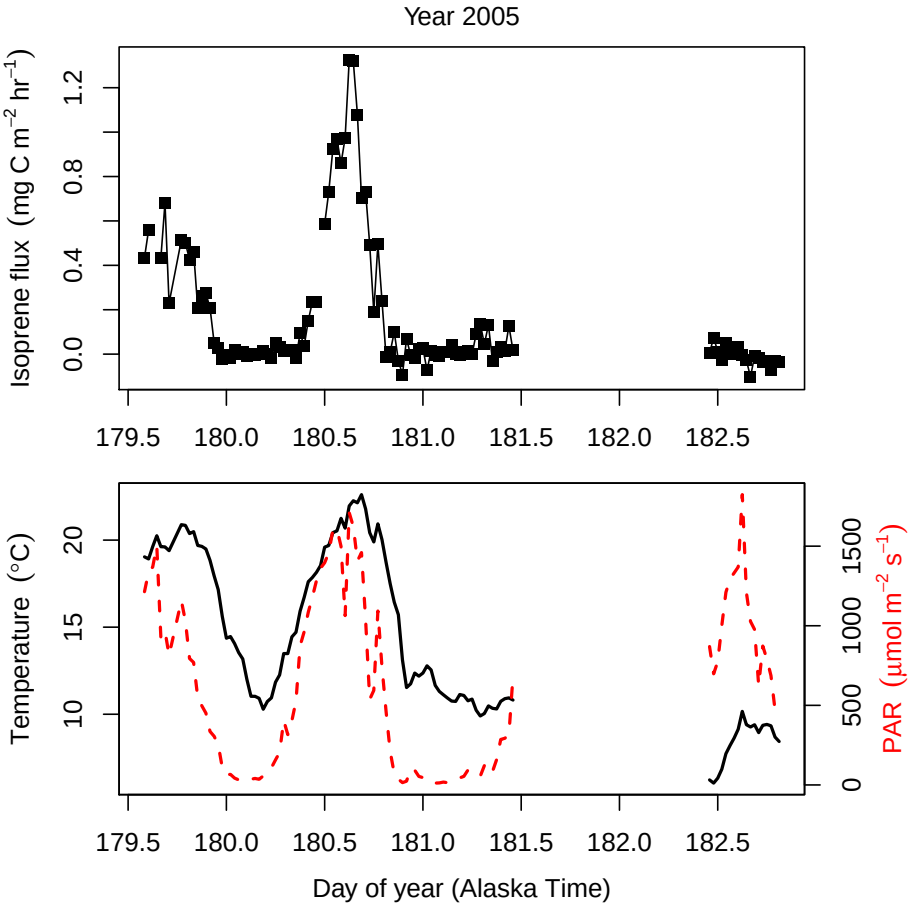

Fig. 3. Ecosystem-level fluxes of isoprene (top panel) and temperature (black, solid line) and photosynthetically active radiation (red, dashed line) for 2005 (bottom panel). The system was not run from day 181 to 192 since light and temperature were suppressed by ground fog.

BGD
9, 13351–13396, 2012

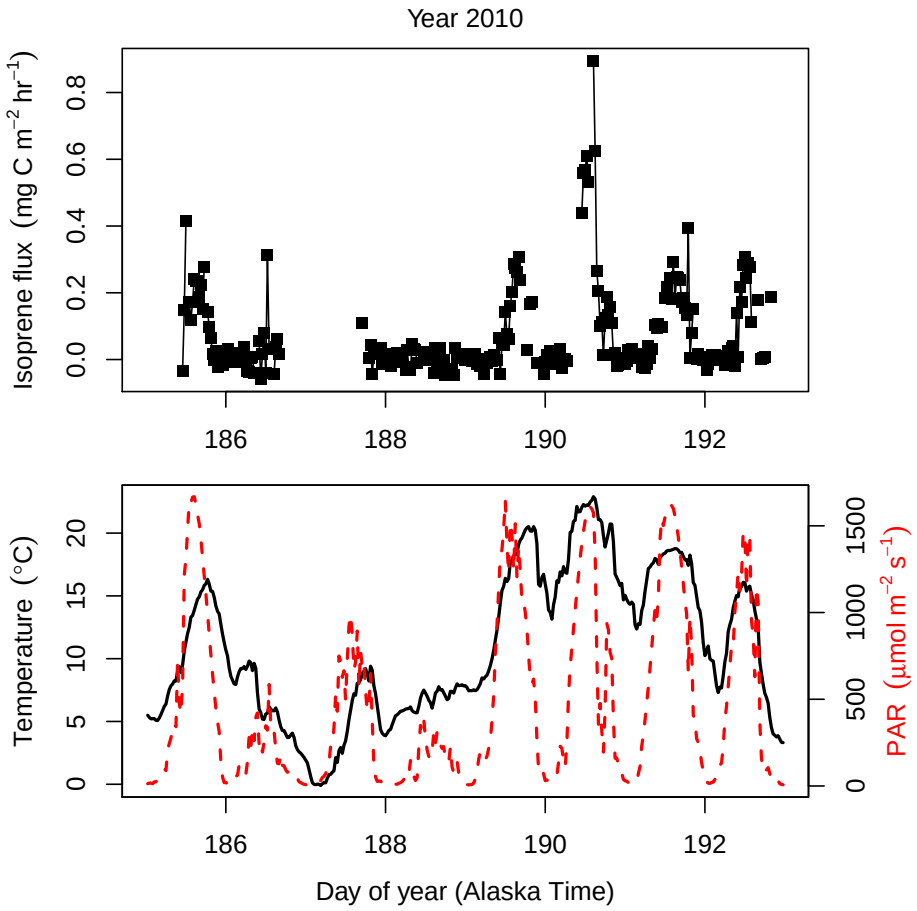

Fig. 4. Ecosystem-level fluxes of isoprene (top panel) and temperature (black, solid line) and photosynthetically active radiation (red, dashed line) for 2010 (bottom panel).

BGD
9, 13351–13396, 2012

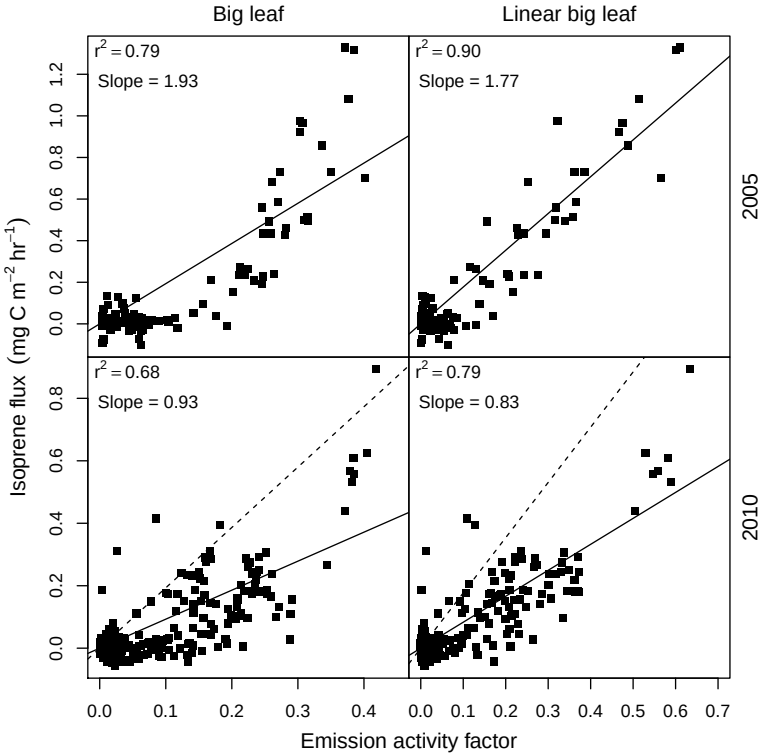

Fig. 5. Left-hand panels: a model of whole-ecosystem isoprene fluxes using the G93 algorithms and treating the tundra as a single "big leaf" for each year (Eq. 5). Model predictions of the EF_{canopy} are on the x-axis and the measurements of whole-system isoprene emissions are on the y-axis. Right-hand panels: the same model (Eq. 5), except the G93 algorithm for light (Eq. 2) has been replaced with a linear version (Eq. 4). The solid line is the linear fit with a zero intercept between the model and the observations. The dashed line in the bottom panels (EC10) is the fit observed in the top panels (EC05), which highlights the inter-annual variability.

BGD
9, 13351–13396, 2012

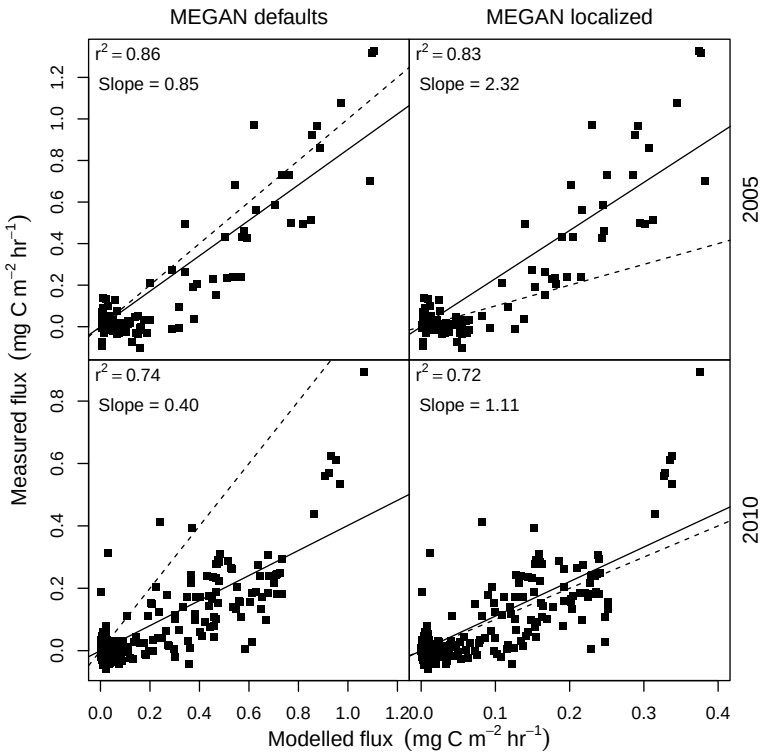

Fig. 6. Comparison of whole-ecosystem isoprene fluxes measured to the MEGAN emission model. Model predictions of the $\text{Emission}_{\text{canopy}}$ are on the x-axis and the measurements of whole-system isoprene emissions are on the y-axis. Left-hand panels: output using the default parameter values from MEGAN's global database. Right-hand panels: output using parameter values estimated for the moist acidic tundra ecosystem. In each panel, the line is the linear fit constrained to a zero intercept and the dashed line is a one-to-one relationship. The top panels are EC05 and the bottom panels are EC10.

BGD
9, 13351–13396, 2012

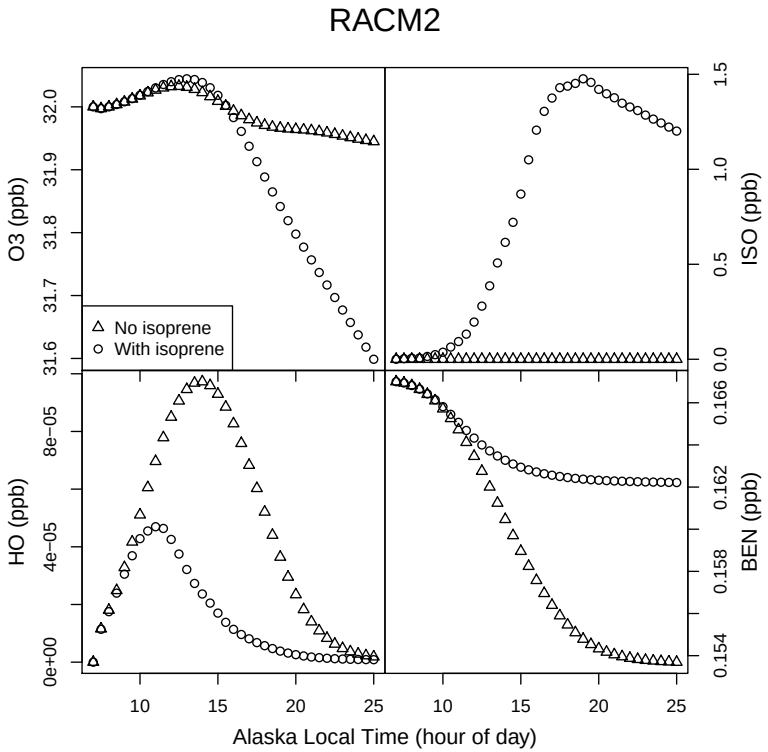

Fig. 7. Results from running a photochemical box model (RACM2) with (circles) and without (triangles) isoprene emissions. The model was driven with the isoprene emissions observed on day of year 180 during EC05. The model time domain reached day 01:00 local time on day of year 181, which is displayed as hour 25. Species codes: O3 is ozone (O_3), HO is the hydroxyl radical, ISO is isoprene and BEN is benzene (C_6H_6). Note that solar noon occurs around 14:00 local time.

BGD
9, 13351–13396, 2012